Electronic Supplementary Material (ESI) for Journal of Materials Chemistry C.

Amplifying gas sensor performance by embedding a cellulose-based buffer layer in organic transistors

Moonjeong Jang,‡[a] Seong Ku Kim,‡[ab] Juyeon Lee,[ac] Seulgi Ji,[a] Wooseok Song,[a] Sung Myung,[a] Jongsun Lim,[a] Sun Sook Lee,[a] Ha-Kyun Jung,[a] Jiseok Lee*[d] and Ki-Seok An*[a]

[a]Thin Film Materials Research Center, Korea Research Institute of Chemical Technology (KRICT), 141 Gajeong-ro, Yuseong-gu, Daejeon 34114, Republic of Korea

[b]Department of Advanced Materials and Chemical Engineering, Hannam University, Daejeon 34430, Republic of Korea

[c]Department of Material Science and Engineering, Korea Univesity, Seongbuk-gu, Seoul 02841, Republic of Korea

[d]School of Energy and Chemical Engineering, Ulsan National Institute of Science and Technology (UNIST), 50 UNIST-gil, Ulsan 44919, Republic of Korea

*Corresponding author. Email: jiseok@unist.ac.kr or ksan@krict.re.kr

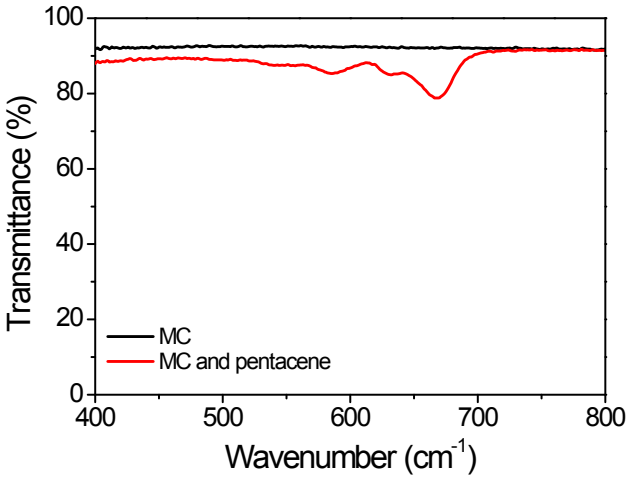

Figure S1. Optical transmittance of MC and MC/pentacene composite film at different wavelengths.

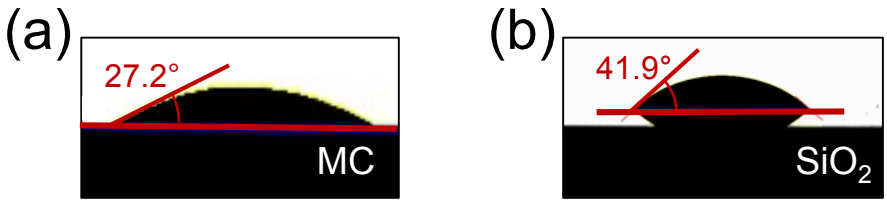

Figure S2. The contact angle observed between water and (a) MC layer and (b) SiO_2 surface.

The contact angle could provide some important information about the surface energy of the material. For this reason, the surface energies (especially hydrophilicity of the surface) of SiO_2 with and without the MC buffer layer was measured and compared using the contact angle experiment. When water was dropped on top of MC layer, low contact angle of 27.2° was observed, which indicates that very hydrophilic surface (with high surface energy) was formed due to the thin MC layer. On the other hand, the surface of SiO_2 exhibited a contact angle of 41.9°. When comparing two surfaces, it is clear that the surface with MC layer is more hydrophilic (with higher surface energy).

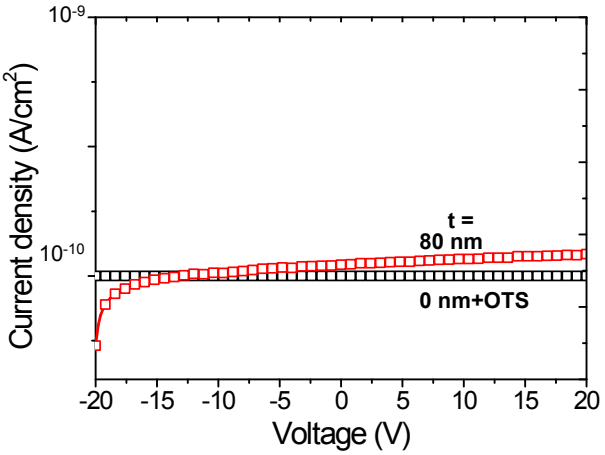

Figure S3. Current density-voltage characteristics of the OTS-SiO_2 (300 nm) and MC (80 nm)-SiO_2 (300 nm) samples.

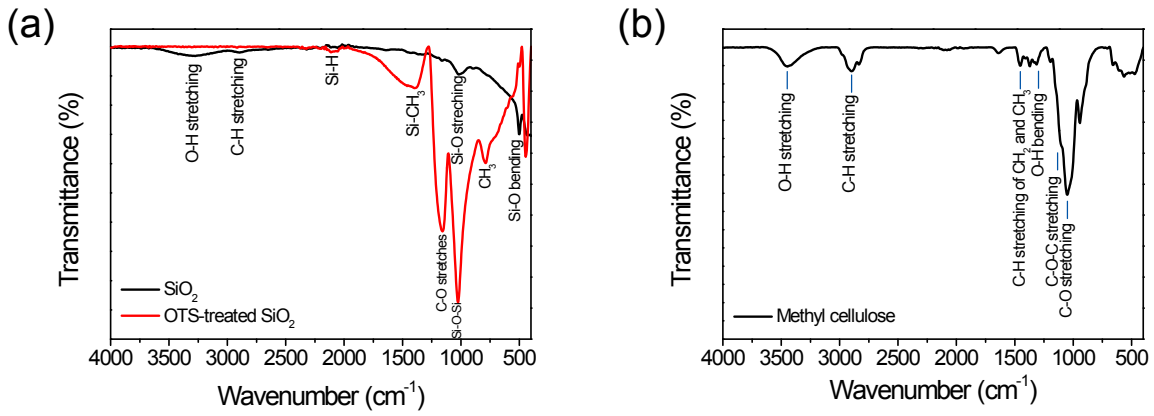

Figure S4. (a) Comparison of FTIR-ATR spectrum of pristine SiO_2 and OTS-treated SiO_2 substrates. (b) FTIR-ATR spectrum of MC powder.

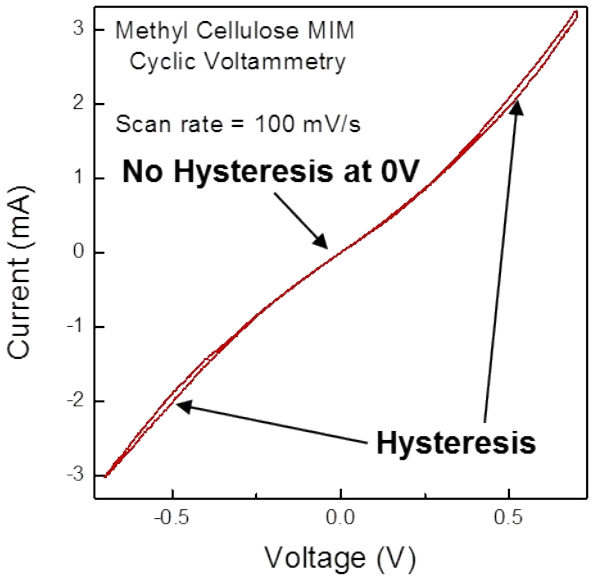

Figure S5. Result of cyclic voltammetry obtained from a MIM device based on methyl cellulose.

A very thin layer (< 100 nm) of methyl cellulose was sandwiched between two metallic electrodes to obtain cyclic voltammogram. Shape and characteristics of the hysteresis occurred during cyclic voltammetry indicate that methyl cellulose dielectric layer polarizes by orientational alignment of dipolar functional groups. As observed in Figure S5, the methyl cellulose MIM does not show any hysteresis behavior at V = 0 V, indicating that dipoles of hydroxyl functional groups are not aligned. However, even with application of small voltages, alignment of dipoles occur; thus, the hysteresis behavior representing dipole polarization can be observed.[1]

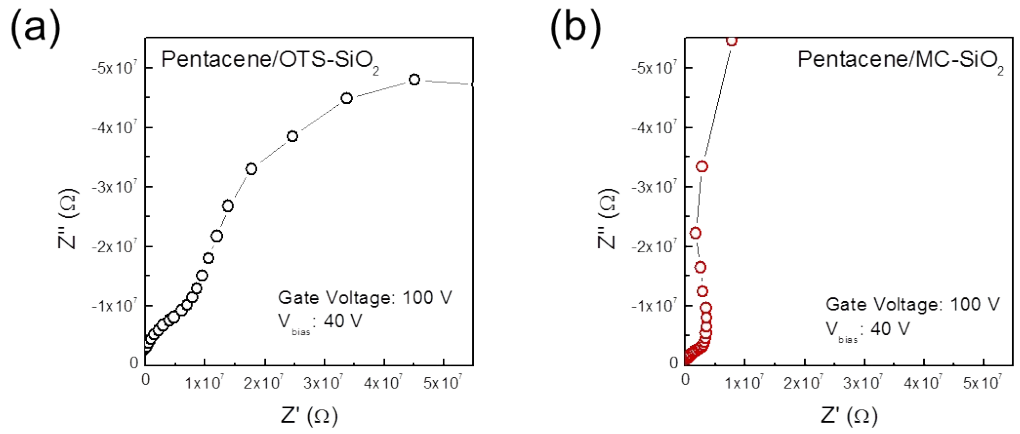

Figure S6. Nyquist plots obtained using ac-impedance measurement with applied gate voltage for pentacene (a) without MC and (b) with MC.

Nyquist plots are obtained from pentacene with and without methyl cellulose (MC). In this case, a gate voltage of 100 V is applied during the impedance measurement. For both Nyquist plots, clearly distinguished bulk and grain boundary semi-circles could be observed. The impedance measurements were performed with gate voltage to ensure that low current observed from the transfer characteristics of pentacene with MC is still caused by grain boundaries. Clearly, the portion of grain boundary resistance is still profoundly larger in comparison with the bulk resistance. Thus, we can easily conclude that any significant change in electrical properties during sensing with gate voltage is also mainly caused at the grain boundaries of pentacenes.

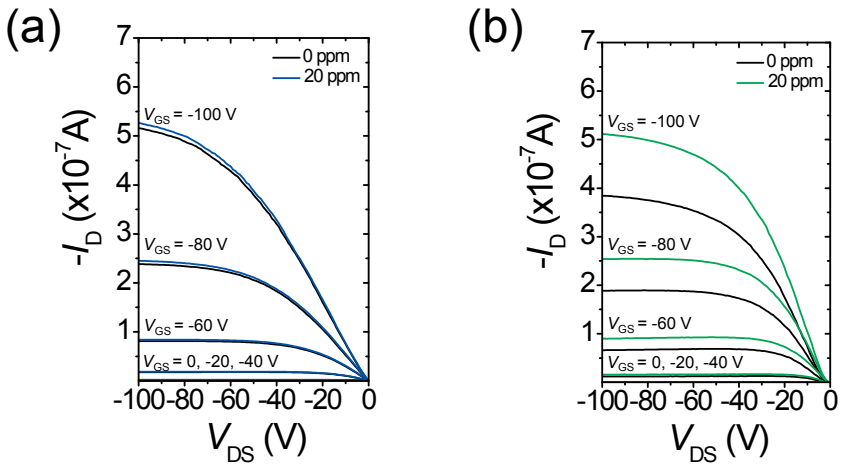

Figure S7. Output characteristics of the pentacene OFET-based sensors (a) without and (b) with MC toward 20 ppm NO_2 gas flow.

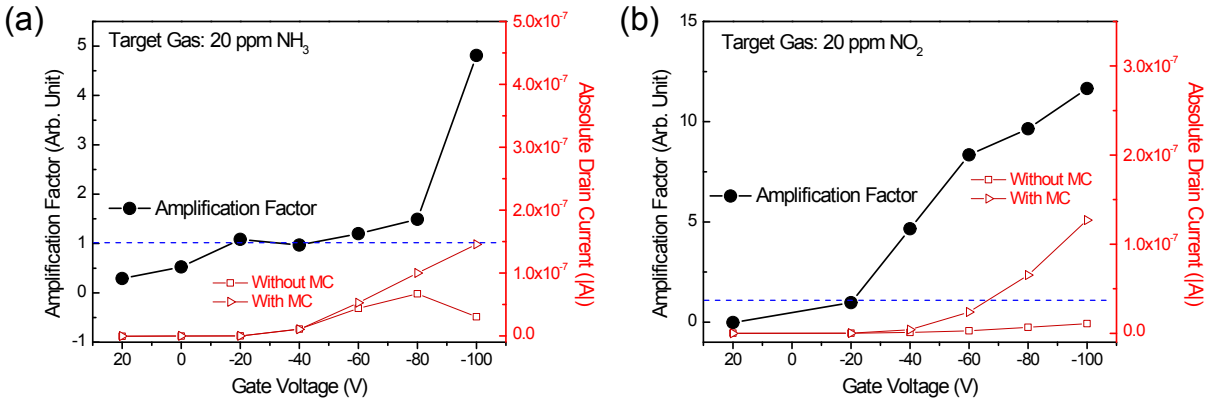

Figure S8. Calculated amplification factors (ratio between drain current observed from pentacene with MC buffer and without MC buffer) for different analytes: (a) NH_3 and (b) NO_2. The absolute drain currents (absolute value of $I_{D,20\ ppm\ gas}$-$I_{D,no\ gas)}$ at different gate bias are also included in the plots.

Figure S8 includes the amplification factors (the ratio between drain currents of pentacene sensors with and without MC buffer layer) and absolute drain currents observed from different target gases (NH_3 and NO_2). For both cases, we could observe significant increase of the amplification factors upon increasing the strength of applied gate potential. At -100 V, amplification factor of MC buffer was about 5 when sensing 20 ppm NH_3 and more than 12 for NO_2; thus, observed amplification factors demonstrates the effectiveness of the MC buffer layers. It is also very interesting to see that amplification factor more than 1 is observed almost as soon as enough gate voltage to active the device is applied for both cases.

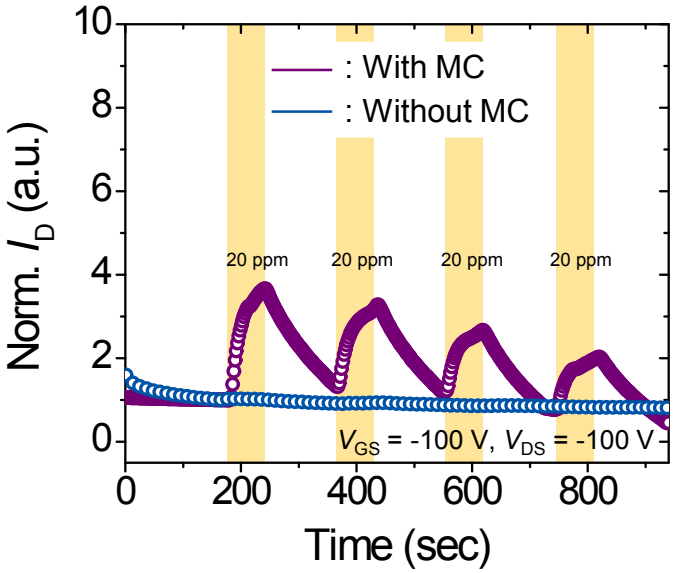

Figure S9. Real-time responses of the sensors with and without MC toward 20 ppm NO_2 gas flow in a saturated humidity atmosphere.

References

1 S. Bonardd, V. Moreno-Serna, G. Kortaberria, D. Díaz Díaz, A. Leiva and C. Saldías, *Polymers*, 2019, **11**, 317.